Editors: Tom Marchioro, march@borg.chem.washington.edu
Denis Donnelly, donnelly@siena.edu

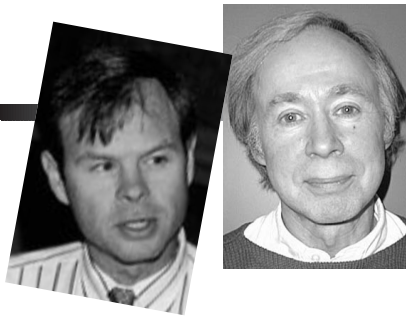

COMPUTER-SIMULATED FRESNEL DIFFRACTION USING THE FOURIER TRANSFORM

By Seymour Trester

THE STUDY OF FRESNEL DIFFRACTION IS AN INTEGRAL PART OF ANY COURSE IN PHYSICAL OPTICS. FRESNEL DIFFRACTION OCCURS WHEN AN APERTURE IS ILLUMINATED WITH COHERENT LIGHT AND THE RESULTING DIFFRACTION PATTERN appears on a screen a finite distance from the aperture. In general, the techniques found in standard optics texts[1] to compute the intensity of the diffraction pattern as a function of position on the screen are limited and aperture-specific. For example, the Fresnel diffraction due to a circular aperture is usually treated in terms of Fresnel zones, whereas the diffraction due to a straight edge is calculated using the Cornu spiral.

However, as texts on modern optics show, we can formulate Fresnel diffraction in terms of the Fourier transform of a modified aperture function.[2] In this article, I present a generalized method, using the Fourier transform, for computing and graphically displaying the Fresnel diffraction intensity pattern for any planar aperture. With the advent of the PC and packaged mathematical software containing the fast Fourier transform algorithm, it is now possible to perform these calculations with minimum effort.[3,4] The advantage of this method is that you can obtain the entire pattern at once, in contrast to the standard methods' point-by-point evaluation process.

In the standard notation used in optics, a spherical light wave of wavelength λ emanating from a single point source is represented by its electric field component; in complex notation, this can be written as $E(r, t) = (a/r)e^{j(kr - \omega t)}$. In this expression, r is the distance from the point source to the point P in space where the field is to be evaluated, k is $2\pi/\lambda$, i is $\sqrt{-1}$, ω is the angular frequency of the wave, t is time, and a is a constant related to the strength of the point source. Of course, the physical field is the real part of the complex $E(r, t)$. One advantage of using complex notation occurs in problems where monochromatic light waves from two or more separated coherent point sources interfere at a point in space. In this case, all the individual fields that are to be summed have the same time factor $e^{-i\omega t}$. We can show that the observable time-averaged light intensity at a point in space is proportional to the square of the absolute value of the resultant field, E_R, at that point.[5] For problems that deal only with relative intensity, the proportionality constant can be taken to be unity, and we have $I = |E_R|^2$. Hence, in the calculation of the resultant intensity at a point in space due to a distribution of point sources, only the spatial part of the field $E(r) = (a/r)e^{ikr}$ for each point source need be considered, because the phase factor containing the time, $e^{-i\omega t}$, squares to unity.

General theory

Consider the situation shown in Figure 1, where an aperture in an opaque plane is illuminated from the left by monochromatic coherent light of wavelength λ. Let $E_{inc}(x_o,y_o)$ be the electric field amplitude of the incident light at the point x_o,y_o in the aperture plane. The distance r from a point x_o,y_o in the aperture plane to a point P on the screen whose coordinates are x,y is given by $r = [z_o^2 + (x_o - x)^2 + (y_o - y)^2]^{1/2}$, where z_o is the distance from the aperture plane to the screen. The problem in diffraction is to compute the resultant electric field E_R at a point P due to the light emanating from each point of the illuminated aperture. Following the treatment of diffraction theory presented by Joseph Goodman,[2] we consider the diffraction that occurs when $z_o^2 >> (x_o - x)^2 + (y_o - y)^2$. This is the case when the aperture and viewing-area dimensions on the screen centered about the z-axis are both much less than the distance between the aperture plane and the screen. This is the typical situation for observing Fresnel diffraction. In this case, we are considering only light waves that are traveling almost parallel to the z-axis. This makes the obliquity factor[1,2] found in the general theory of diffraction equal to unity. The resultant electric field of the light at a point P is then given by the mathematical expression of the Huygens-Fresnel principle

Helping Students Map Electric Potentials and Fields Quickly and Efficiently

By Christopher Bracikowski, Richard Schneider, and Joseph Singley

Recently, an article by Richard A. Young[1] described an experiment to produce beautiful and illustrative 3D graphs of electric potential surfaces using the standard electric field mapping apparatus (available from Pasco Scientific, Roseville, Calif.). In summary, a conductor arrangement is painted onto a sheet of conductive paper. The conductors are connected to the terminals of a power supply to maintain a constant potential difference between them. This creates an electric field and an electrostatic potential gradient in the space surrounding the conductors. In his article, Young described a fast, automated procedure for collecting the electrical potential data using an *x-y* recorder controlled by a Labview program. In this experiment, the student is a passive observer as the *x-y* recorder quickly moves a probe over the paper, recording 200 potential data points per minute.

In 1997, an article by Jim Horn[2] described a method of manually collecting and analyzing the potential versus position data. The electric potential in the paper plane around the conductors is measured manually at all points on a 28-cm × 20-cm grid with a probe connected to a voltmeter, and then the data is entered into Microsoft Excel by hand. However, measuring and entering all 609 data points manually is quite a laborious and time-consuming process. Indeed, Horn states that students are hard pressed to complete all measurements and enter the data into Excel in a single one-hour class period.

The techniques described in these two articles represent two extremes. One technique is fast, but does not involve students at all. The other technique involves students directly, but takes too long. We have developed an alternative experimental technique that is a compromise between maximizing speed on the one hand and student involvement on the other.

We have streamlined Horn's data acquisition and data entry processes by running Windows 95 with Excel 7.0 and LoggerPro 1.0.3 connected to a Universal Laboratory Interface (available from Vernier Software, Portland, Oregon). We use the ULI's standard voltage probes to probe the electrostatic potential produced by a conductor arrangement painted on conductive paper. In this experiment, the computer serves as a digital voltmeter to make the data acquisition easier. Students manually measure values of electric potential along one column of grid points using the ULI and LoggerPro. This column of data is then copied from LoggerPro and pasted into Excel. The procedure is repeated for each column of grid points. With this technique, the entire experiment from data acquisition to 3D graphing can be completed in about half an hour.

We have also developed a similar technique to measure and graph the vector magnetic field of a magnet as a function of position. We place a magnet on the same grid paper as mentioned earlier. We then use the ULI with its magnetic field probe to measure the *x* and *y* components of the magnetic field vector at each point on the grid (actually we use every other column so that the vector arrows do not overlap when graphed). This Hall effect magnetic-field probe measures the component of the magnetic field perpendicular to its surface. By orienting the probe in the *x* and *y* directions respectively, we can determine the two orthogonal components of the magnetic field at each grid location. We copy the magnetic field components at each grid point from LoggerPro into Stanford Graphics (available from Visual Numerics, Houston, Texas), then produce a vector plot of the magnetic field vectors at all grid points.

We would be happy to provide detailed instructions for these experiments, specifically the configurations for LoggerPro, upon request.

References

1. R.A. Young, "Electric-Field Mapping Revisited," *Computing in Physics*, Vol. 12, No. 5, Sept./Oct. 1998, pp. 432–439.
2. J. Horn, "Electrostatic Landscapes," *The Physics Teacher*, Vol. 35, Nov. 1997, pp. 499–501.

Christopher Bracikowski is an associate professor of physics, Richard Schneider is a physics student, and Joseph Singley is a physics major, all at Bloomsburg University in Bloomsburg, PA 17815. They can be reached at brac@bloomu.edu.

$$E_R(x,y) = C\int_{-\infty}^{+\infty}\int_{-\infty}^{+\infty} E_{inc}(x_o,y_o)A(x_o,y_o)\left(\frac{\exp(ikr)}{r}\right)dx_o dy_o, \quad (1)$$

where C is a constant and $A(x_o,y_o)$ is the aperture plane's amplitude transmission function. The function $A(x_o,y_o)$ gives the fraction of the incident field transmitted at each point of the aperture plane. At those points x_o,y_o where the plane is opaque, $A(x_o,y_o) = 0$, and where the plane is completely transparent, $A(x_o,y_o) = 1$.

You can find an excellent detailed discussion of scalar diffraction theory and Kirchhoff's derivation of Equation 1 from first principles in Chapter 3 of Goodman's book.[2] There it is shown that the constant is given by $C = -i/\lambda$. That Equation 1 is an ex-

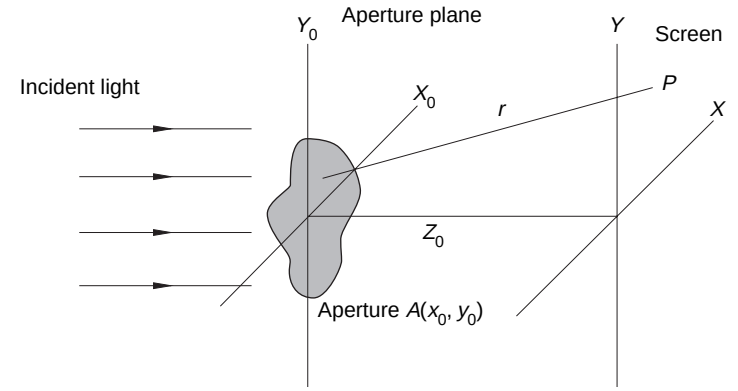

Figure 1. Monochromatic coherent light coming from the left illuminates an aperture in an opaque plane.

pression of the interference of Huygens' secondary wavelets can be seen as follows. Huygens' principle states that each point on a wavefront can be considered a new point source of light emitting secondary spherical waves. Fresnel surmised that the diffraction of light is due to the interference of these secondary waves. The term $E_{inc}(x_o,y_o)A(x_o,y_o)$ represents the field transmitted by the aperture at the point x_o,y_o; when multiplied by the factor $(\exp(ikr))/r$, the term yields the contribution of the spherical wave emanating from the point source at x_o,y_o to the field at point P on the screen. By integrating over the x_o,y_o coordinates of the aperture plane, we are superimposing the field contributions of all the point sources comprising the aperture—which yields the resultant field E_R at the point P.

We can simplify Equation 1 by making use of the paraxial ray condition, $z_o^2 >> (x_o - x)^2 + (y_o - y)^2$. First, the expression for r is rewritten as $r = z_o\{1 + [(x_o - x)^2 + (y_o - y)^2]/z_o^2\}^{1/2}$. The square root term is then approximated by the first two terms of a binomial expansion, yielding $r \approx z_o + [(x_o - x)^2 + (y_o - y)^2]/2z_o$. Furthermore, expanding the quadratic terms yields $r \approx z_o + (x^2 + y^2)/2z_o + (x_o^2 + y_o^2)/2z_o - (xx_o + yy_o)/z_o$. We will use this expression for r in the exponential of Equation 1, where, due to the large value of k, the phase kr is sensitive to small changes in r. However, these changes will not appreciably affect the denominator, where r can be approximated by z_o. Making these substitutions into Equation 1, we get

$$E(x,y) = C_2 \int_{-\infty}^{\infty}\int_{-\infty}^{\infty} \left\{E_{inc}(x_o,y_o)A(x_o,y_o)\exp[(ik/2z_o)(x_o^2+y_o^2)]\right\} \exp[(-ik/z_o)(xx_o+yy_o)]dx_o dy_o, \quad (2)$$

where $C_2 = (-i/\lambda z_o)\exp(ikz_o)\exp[(ik/2z_o)(x^2 + y^2)]$. Examination of Equation 2 shows that the diffraction field $E(x,y)$ is related to the Fourier transform of a modified aperture plane transmission function, $M(x_o,y_o)$, where

$$M(x_o,y_o) = E_{inc}(x_o,y_o)A(x_o,y_o)\exp[(ik/2z_o)(x_o^2 + y_o^2)]. \quad (3)$$

To find the field at a point P on the screen whose coordinates are x,y, the Fourier transform of $\boldsymbol{M}$ must be evaluated at the spatial frequencies $x/\lambda z_o$ and $y/\lambda z_o$. Equation 2 will serve as the basis for the computer simulation of Fresnel diffraction presented later, when I evaluate the Fourier transform at spatial frequencies that automatically satisfy the conditions described earlier.

Computer simulation

I performed the calculations presented here using Mathcad 7.0, a commercial mathematical software package for Windows developed and sold by MathSoft. Using the fast Fourier transform algorithm, Mathcad can calculate the 2D discrete Fourier transform of data that is presented in matrix form. The Mathcad operator for this procedure is denoted by *icfft*(***M***), where ***M*** is a matrix. For the case where ***M*** is an $N \times N$ square matrix whose elements are M_{y_o,x_o}, the *icfft* operator returns an $N \times N$ matrix whose elements are given by

$$[icfft(\mathtt{M})]_{y,x} = (1/N)\sum_{x_o=1}^{N-1}\sum_{y_o=1}^{N-1}(\mathtt{M}_{y_o,x_o})\exp[(-i2\pi/N)(xx_o+yy_o)], \quad (4)$$

where x_o, y_o, x, and y are indices that go from 0 to $(N - 1)$ in integer steps. The x_o, y_o indices are the coordinates for points on the aperture plane whereas the x, y indices are those for points on the screen. Note that, for these matrices, the y coordinate is the row index and x is the column index. Thus, when these matrices are displayed graphically as they will be, the x and y axes will each have their usual orientation.

To construct an $N \times N$ matrix to represent the modified aperture function $M(x_o,y_o)$ given by Equation 3, we first define an aperture plane transmission matrix whose elements A_{y_o,x_o} are made equal to zero where the plane is opaque and made equal to one where the plane is transparent. According to Equation 3, we should then multiply each element A_{y_o,x_o} by the factor $\exp[(ik/2z_o)(x_o^2 + y_o^2)]$. However, what k and z_o values should be used in the exponential? To answer this question we note that the computer evaluation of the Fourier transform of ***M***, as given by Equation 4, is at the frequencies x/N and y/N. As stated earlier, to compute the diffraction field given by Equation 2 at a point P on the screen whose coordinates are x, y, you must evaluate the Fourier transform at frequencies $x/\lambda z_o$ and $y/\lambda z_o$. Thus, if the prod-

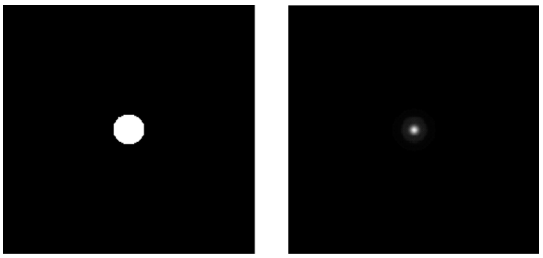

Figure 2. (a) Circular opening comprised of the first Fresnel zone. That is, the opening has a radius *R* of $\sqrt{N}$ in an $N \times N$ aperture plane. The case shown is for $N = 256$. (b) This simulated Fresnel diffraction intensity pattern results when the aperture plane shown in (a) is illuminated by a plane wave at normal incidence.

uct of λz_o is taken to be equal to N, the computer-evaluated Fourier transform will be at the correct frequencies. The equating of λz_o to N is fundamental to this method of computer simulation. Note that the values of λ and z_o do not have to be separately specified. In addition, the equating of λz_o to N is made with the tacit assumption that $\lambda << z_o$ so that the condition of $z_o^2 >> (x_o - x)^2 + (y_o - y)^2$ used in the derivation of Equation 2 will be satisfied. We can now write

$$\boldsymbol{M}_{y_o,x_o} = (E_{inc})_{y_o,x_o} A_{y_o,x_o} \exp[(i\pi/N)(x_o^2 + y_o^2)]$$

where the matrix elements $(E_{inc})_{y_o,x_o}$ give the amplitude of the incident light illuminating the aperture plane at the point x_o,y_o. In this article, we consider the case of the aperture being illuminated by a plane wave traveling parallel to the z-axis, as shown in Figure 1. This is the situation where the aperture is directly illuminated by light from a laser. In this case, the amplitude of the incident field is a constant over the aperture plane, and we will take the matrix elements $(E_{inc})_{y_o,x_o}$ all equal to one.

After forming the matrix $\boldsymbol{M}$, we are now in position to simulate computationally the diffraction field $E(x,y)$ given by Equation 2. This is done by computing the matrix elements

$$E_{y,x} = \{-i\exp(ikz_o)\exp[(i\pi/N)(x^2 + y^2)]\}[icfft(\boldsymbol{M})]_{y,x} \quad (5)$$

where we again replace λz_o by N. Note also that the factor $1/\lambda z_o$ that appears in the coefficient C_2 of Equation 2 is accounted for by the factor $1/N$ of the *icfft*($\boldsymbol{M}$) operation. For the most part we will be interested in computing the relative light intensity distribution on the screen, which is given by the matrix elements $I_{y,x} = |E_{y,x}|^2$. Hence, the phase factor in the curly brackets of Equation 5 squares to unity and the value of the product kz_o does not have to be specified. This yields

$$I_{y,x} = |[icfft(\boldsymbol{M})]_{y,x}|^2. \quad (6)$$

Applying the method

To illustrate this method, we now use it to computer-simulate the Fresnel diffraction pattern for various apertures. These calculations will of course utilize the equations derived earlier, where the geometry is such that the paraxial ray approximation, $z_o^2 >> (x_o - x)^2 + (y_o - y)^2$ is valid and makes the obliquity factor unity. Hence, these computer simulations should be compared only to the results of experiments that meet this condition.

Circular openings and circular apertures. To treat the problem of diffraction by a transparent circular opening of radius R in an otherwise opaque aperture plane, we first define an $N \times N$ transmission matrix to represent $A(x_o, y_o)$, the transmission function of the aperture plane. We do this by using the conditional If statement of Mathcad 7.0 and define the matrix elements A_{y_o,x_o} as

$$A_{y_o,x_o} = if([(x_o - x_c)^2 + (y_o - y_c)^2] \le R^2, 1, 0) \quad (7)$$

where the position indices x_o and y_o go from 0 to $N - 1$ in integer steps. The If statement defines a circular opening in the aperture plane of radius R centered at the point $x_o = x_c$, $y_o = y_c$. That is, the matrix elements A_{y_o,x_o} are defined as 1 for those points in the aperture plane that lie in this circle and 0 for those points outside it. Using the surface plot capabilities of Mathcad, it is possible to obtain a computer graphic of a matrix. The graphics software establishes an $N \times N$ grid of the x_o,y_o coordinates in the plane of the page. The origin of the coordinates, the point where $x_o = 0$ and $y_o = 0$ is at the upper left-hand corner of the grid, and we orient the x_o axis so that it is horizontal with increasing values to the right. The y_o-axis is perpendicular to this direction with increasing values down the grid. Recall that the x_o and y_o indices are the matrix element's column and row indices respectively; thus, with this orientation of the axes, the position of a matrix element in the matrix and on the grid are the same. The value of each matrix element is displayed as a shade of gray at its x_o,y_o position on the grid. The largest value is in white and the smallest in black. The computer graphic for the matrix $\boldsymbol{A}$ defined earlier is shown in Figure 2a. For this matrix, the values of N and R^2 were both taken to be 256 with the center of the circular opening at $x_c = 128$, $y_c = 128$.

We now compute the Fresnel diffraction pattern that results on a screen at a distance z_o from the aperture plane for the case where this circular opening is illuminated by a plane wave of amplitude $E_{inc} = 1$. To do this, we form the matrix $\boldsymbol{M}$, discussed earlier, where the elements $M_{y_o,x_o} = A_{y_o,x_o}\exp[(-i\pi/N)(x_o^2 + y_o^2)]$. The Fourier transform operator *icfft* is then applied to this matrix. The matrix elements $I_{y,x} = |[icfft(M)]_{y,x}|^2$, which give the relative intensity of the diffraction pattern at each point x,y on the screen, are then computed. The graphic of the matrix $\boldsymbol{I}$ is shown in Figure 2b.

It is interesting to compare the above method, which

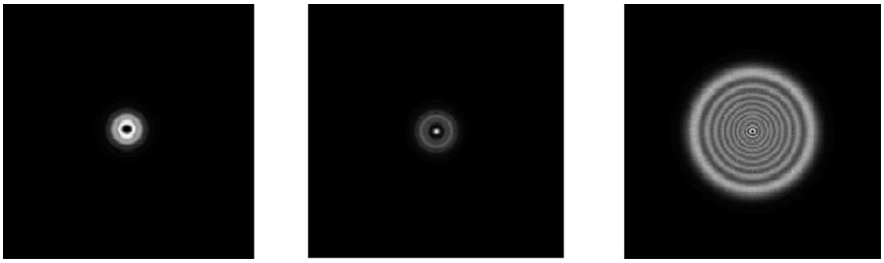

Figure 3. Simulated diffraction intensity patterns for circular openings comprised of (a) two, (b) three, and (c) 20 Fresnel zones.

quantitatively gives the intensity at all points on the screen, with that of the semiquantitative standard treatment of Fresnel diffraction by a circular opening.[1] In that treatment, the only point for which the intensity can be calculated easily is the point P_c on the screen that lies on the circle's axis, that is, the point whose screen coordinates are $x = x_c$, $y = y_c$. In that method, the opening, illuminated at normal incidence by a plane wave, is divided into a set of concentric circles whose radii are given by the relation $R_m^2 = m\lambda z_o$ where $m = 1,2,\ldots$, and R_m is the radius of the mth circle. The annular regions between successive circles are called Fresnel half-period zones. The radii R_m are such that points in the $m + 1$ zone are, on average, a distance $\lambda/2$ farther from P_c than the corresponding points in the mth zone are from P_c. The surprising result from the analysis is that if an integral number of zones exactly fill the circular opening, then the resultant intensity at P_c is approximately zero if the integer is even, and approximately four times the unobstructed intensity when the integer is odd. The reason is this: it can be shown that the contribution to the field at the point P_c from the first zone is twice that of the unobstructed field and that the total contribution from two adjacent zones yields zero, because individually their fields are approximately equal in magnitude and out of phase by $\lambda/2$.

The radius of the circular opening shown in Figure 2a is for $R^2 = 256$, which is $1 \times N$. Recall that in this computer simulation method we use $\lambda z_o = N$, hence $R^2 = \lambda z_o$, which means that one zone fills the opening. As seen from Figure 2b, the intensity at the point P_c, which is in the center of the circular diffraction pattern, is bright. Furthermore, the computed value for the matrix element $I_{128,128}$, which gives the intensity at point P_c, is 3.999. Because the amplitude of the incident plane wave illuminating the aperture is $E_{inc} = 1$, the unobstructed intensity at all points on the screen is also 1. Hence, the earlier-computed value $I_{128,128}$ is in good agreement with the results of the zone treatment of diffraction discussed earlier.

I repeated the computer-simulated diffraction calculations for three other circular openings. The radius R of the first opening satisfies the relation $R^2 = 2N = 2\lambda z_o$, so the first two Fresnel zones comprise the aperture. For the second opening, $R^2 = 3N = 3\lambda z_o$, so three zones fill the aperture; for the third opening, $R^2 = 20N = 20\lambda z_o$, so 20 zones fill the aperture. The resulting intensity matrix $\boldsymbol{I}$ for each is shown in Figures 3a, 3b, and 3c. These computer-simulated diffraction patterns are in excellent agreement with the experimental results for apertures of corresponding radii shown elsewhere.[1]

To further show the accuracy of this computer simulation method, it is interesting to compute the phase of the resultant field at the point P_c for the case of a circular opening. We do this by evaluating the matrix element $E_{y,x}$ given by Equation 5 at the point $x = x_c$, $y = y_c$. For the circular opening shown in Figure 2a, N equals 256 and point P_c has the coordinates $x_c = 128$, $y_c = 128$, so the matrix element $E_{128,128}$ according to Equation 5 is $-i\exp(ikz_o)[icfft(M)]_{128,128}$. This can be written as $E_{128,128} = E_o e^{-i\pi/2}[icfft(M)]_{128,128}$ where $E_o = \exp(ikz_o)$ is the field of the unobstructed unit amplitude incident plane wave at the screen a distance z_o from the aperture plane. For this circular opening comprised of a single zone, that is, whose $R^2 = \lambda z_o$, Mathcad's evaluation of the matrix element $[icfft(M)]_{128,128}$ yields $2e^{1.557i}$. Because 1.557 is within 1% of $\pi/2$, $E_{128,128}$ is approximately $2E_o$, which means that the resultant field at P_c due to the first zone is in phase with the unobstructed field E_o and has twice its amplitude. This is clearly seen by drawing the vibration curve for a circular aperture, using phasors.[1] This phasor addition confirms the result just calculated for the first zone. Moreover, the vibration curve also shows that the resultant field at P_c from points in each succeeding zone has an additional phase of π. Similarly, using this method of computer simulation, you can show that the phase of the resultant field at P_c due to points in the second zone is out of phase with that due to the first zone by π and is approximately of the same magnitude. That is, for the second zone $E_{128,128} = 2E_o e^{i\pi}$.

One last comment concerning the field at P_c should be made. The earlier calculation shows that the resultant field at P_c due to the first zone is in phase with the unobstructed incident field at this point. However, the vibration curve shows that this resultant field is $\pi/2$ out of phase with the field at P_c emanating from a point in the center of the first zone. Hence, this field from the center point is $\pi/2$ out of phase with that of the unobstructed field. This curious phase difference is not accounted for in Fresnel's formulation of Huygens' Principle, where it is assumed that the fictitious sources emitting the secondary wavelets are in phase with the primary wave. However, Equation 1, which results from Kirchhoff's derivation of the Huygens-Fresnel principle using the wave equation for light, contains the constant $C = -i/\lambda$. This shows that the $\pi/2$ phase difference between

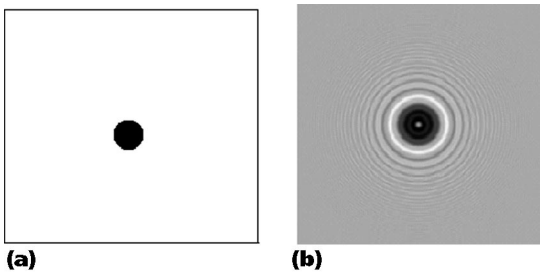

Figure 4. (a) A circular obstacle of radius $R = \sqrt{N}$ in the center of an $N \times N$ transparent aperture plane for which $N = 256$. (b) Its simulated diffraction pattern. Note the bright spot in the center of the pattern.

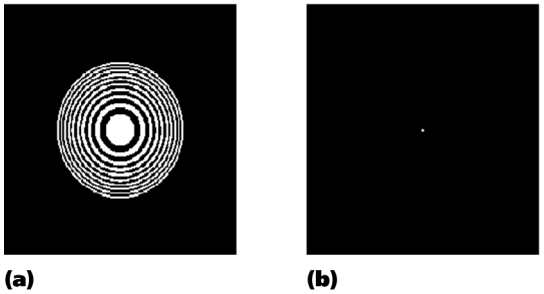

Figure 5. (a) Fresnel zone plate with the first 10 odd-numbered zones made transparent. (b) The simulated diffraction pattern for (a) when illuminated by a plane wave at normal incidence.

the secondary wavelets and the primary wave needed in the Huygens-Fresnel theory diffraction is a natural consequence of the wave nature of light.[1,2]

Using the method I have presented, you can easily calculate the diffraction due to a circular obstacle. For the case of $N = 256$ and thus $R^2 = 256$, $x_c = 128$, and $y_c = 128$, the aperture transmission matrix $\boldsymbol{A}$ is defined as $\boldsymbol{A}_{y_o,x_o} = if([(x_o - x_c)^2 + (y_o - y_c)^2] \le R^2, 0, 1)$ and is shown in Figure 4a. The resulting intensity matrix $\boldsymbol{I}$ is then computed and is shown in Figure 4b. (The details for this calculation are included in the full version of this article; contact the author for more information.) Note that the intensity at the point P_c on the screen lying on the axis of the circular obstacle is bright and evaluating the matrix element at this point yields $I_{128,128} = 1$. This bright spot, known today as Poisson's spot, is a striking example of the diffraction of light waves around an obstacle and their constructive interference in the geometrical shadow of the obstacle.

The longer version of this article also discusses the problem of computer-simulated diffraction for a Fresnel zone plate.[1,6] To effect this simulation, we first construct an $N \times N$ matrix $\boldsymbol{A}$ to represent the transmission function of the zone plate. For a zone plate whose odd-numbered zones are transparent and even opaque, we define

$$A_{y_o,x_o} = \sum_{j=1}^{p} \text{if}\,[2N(j-1) \le (x_o - x_c)^2 + (y_o - y_c)^2 \le N(2j-1), 1, 0\,], \quad (8)$$

where the integer p gives the number of transparent odd zones. The matrix $\boldsymbol{A}$ for the case of $N = 256$, $x_c = 128$, $y_c = 128$, and $p = 10$ is shown in Figure 5a, and the computed intensity matrix $\boldsymbol{I}$ is shown in Figure 5b. Note that it is essentially zero except in the region of the axial point P_c. The intensity at this point is given by $I_{128,128}$, which equals 400. This is 100 times the intensity produced by a single zone and illustrates the focusing ability of the zone plate when illuminated by parallel light. To further illustrate how the zone plate has the characteristics of a thin lens, the longer version of this article contains a computer simulation of the diffraction that occurs when the plate is illuminated by an off-axis point source.

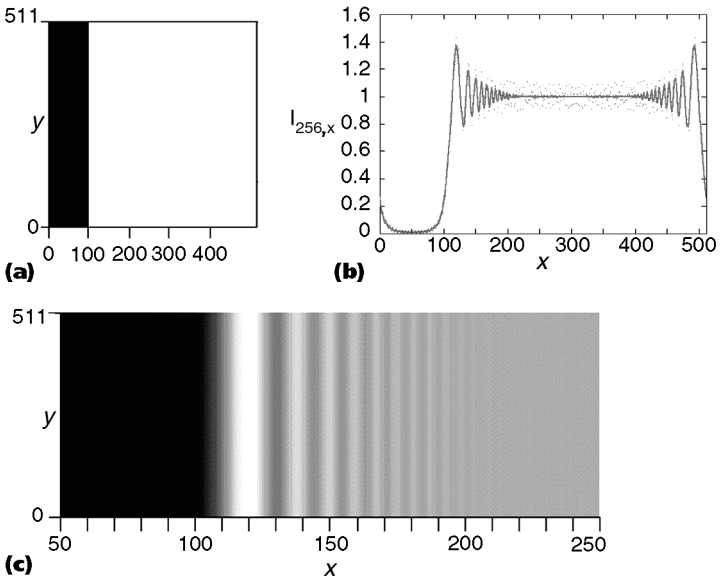

Figure 6. (a) Opaque strip with edges at $x = 0$ and $x = 100$ in a 512×512 aperture plane. (b) Graph of diffraction intensity matrix elements $I_{256,x}$ versus x for strip shown in (a). (c) Simulated diffraction pattern due to the straight edge at $x = 100$ strip in (a).

Straight edge and slits. Despite the advantages of the Fourier transform approach, exercise caution in those cases where an edge of the aperture lies close to a boundary of the aperture plane. In this case, an aliasing effect occurs when computing the diffraction pattern. As an example, consider the computer simulation of Fresnel diffraction due to the straight edge shown in Figure 6a. The matrix elements of $\boldsymbol{A}$ for this 512×512 aperture plane are defined as $A_{y_o,x_o} = 0$ for $x_o = 0, 1, \ldots 100$ and $A_{y_o,x_o} = 1$ for $x_o = 101,$

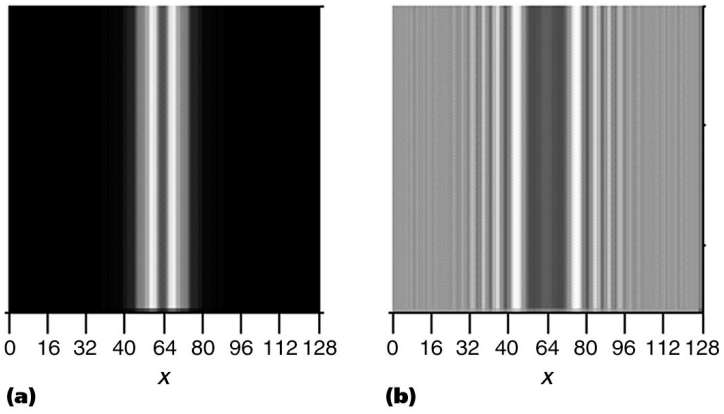

Figure 7. (a) Simulated diffraction pattern for a narrow slit of width $\Delta x = 20$ situated in the center of a 128×128 opaque aperture plane. (b) Simulated diffraction pattern for a narrow rectangular obstacle of width $\Delta x = 3$ situated in the center of a 128×128 transparent aperture plane.

102,…511, where y_o goes from 0, 1,…511. That is, the edge of the opaque portion of the aperture is at $x = 100$. The intensity matrix $\boldsymbol{I}$ for the diffraction pattern is computed in the usual manner and, as one would expect for this aperture, the intensity matrix elements $I_{y,x}$ for a given x do not depend on the y coordinate. In Figure 6b the values of the matrix elements $I_{256,x}$ are plotted versus x and are shown as points. Also shown in this figure is a curve fitted to the data obtained using Mathcad's polynomial regression function. In Figure 6b, the intensity pattern to the right of $x = 100$ is repeated to the left of $x = 511$. This aliasing effect occurs when taking the discrete Fourier transform of a function because the frequencies present in the transform are as if the function were periodic.[7] Hence, the result shown in Figure 6b represents a wide slit whose edges are at $x = 100$ and $x = 511$ with the slit repeating to the left of $x = 0$ and the opaque strip to the right of $x = 511$. (Details and a fuller discussion are available in the long version of this article). Figure 6b should be compared to the intensity calculation for a wide slit obtained using the Cornu spiral.[6] In addition, the surface plot of the intensity matrix $\boldsymbol{I}_{y,x}$ in the region of $x = 50$ to $x = 250$, where no overlap of patterns occurs, is shown in Figure 6c and is found to be in good agreement with an experimentally determined diffraction pattern due to a straight edge.[1,6]

There are two more interesting cases for which the Fresnel diffraction intensity is easily simulated by this computational method: the diffraction due to a long, narrow slit and that due to a long, narrow obstacle. The intensity matrices for a slit of width $\Delta x = 20$ and for a very narrow obstacle of width $\Delta x = 3$, each located in the center of 128×128 aperture planes, are shown in Figures 7a and 7b respectively. The fringes that occur within the geometric image of the slit and in the geometric shadow of the obstacle are evident. Aliasing does not occur in these cases because the edges of the apertures are far from the boundaries of the aperture plane.

The method presented here enables the computer simulation of Fresnel diffraction for almost any planar aperture, using the Fourier transform capabilities of packaged mathematical software. The technique is straightforward, and the computing time using a Pentium PC is inconsequential. The openings and obstacles used in this article's examples were all regularly shaped, so that the aperture plane matrix elements A_{y_o,x_o} could be easily defined. However, the method can be extended to irregularly shaped apertures as well. To do this, you scan a drawing of the aperture and save it as a bitmap file. You can then import this file into Mathcad 7.0 as a matrix of 1's and 0's, which serve as the elements of the aperture matrix $\boldsymbol{A}$. For example, you can use this technique to calculate the diffraction due to a razor blade. You can then compare your results to the experimentally determined pattern found in many elementary physics texts, where it is presented as a paradigm of Fresnel diffraction.

References

1. E. Hecht, *Optics*, 2nd ed., Addison Wesley Longman, Reading, Mass., 1987, Chapter 10.
2. J.W. Goodman, *Introduction to Fourier Optics*, McGraw-Hill, New York, 1968, Chapter 4.
3. S.A. Dodds, "An Optical Diffraction Experiment for the Advanced Laboratory," *Amer. J. Physics*, Vol. 58, No. 7, July 1990, pp. 663–668.
4. R.G. Wilson, S.M. McCreary, and J.L. Thompson, "Optical Transformations in Three-Space: Simulations with a PC," *American J. Physics*, Vol. 60, No. 1, Jan. 1992, pp. 49–56.
5. G.R. Fowles, *Introduction to Modern Optics*, Holt, Rhinehart, and Winston, New York, 1975, p. 59.
6. M.V. Klein, *Optics*, John Wiley & Sons, New York, 1970.
7. H.J. Weaver, *Theory of Discrete and Continuous Fourier Analysis*, John Wiley & Sons, New York, 1989, p. 242.

Seymour Trester is a professor in the Physics Department of C.W. Post Campus, Long Island University, Brookville, NY 11548; strester@liu.edu.